

Nonlinear control of STATCOM for stabilization of synchronous generator

Shubhransu S. Dash⁽¹⁾ and B.K. Panigrahi⁽²⁾

⁽¹⁾Department of Electrical Engineering, College of Engineering, Anna University, Chennai - 600 025, Tamilnadu, INDIA, e-mail: munu_dash_2k@yahoo.com

⁽²⁾Department of Electrical Engineering, University College of Engineering, Burla, Orissa, INDIA

SUMMARY

A Static Synchronous Compensator (STATCOM) is a typical Flexible AC Transmission System (FACTS) device playing a vital role as a stability aid for small and large transient disturbances in an interconnected power system. This paper deals with design and evaluation of a feedback linearizing nonlinear controller for STATCOM installed in a single-machine infinite-bus power system. In addition to the co-ordinated control of AC and DC bus voltages, the proposed controller also provides good damping to the electromechanical oscillation of the synchronous generator under transient disturbances. The efficiency of the control strategy is evaluated by computer simulation studies. The comparative study of these results with the conventional cascade control structure establishes the elegance of the proposed control scheme.

Key words: STATCOM, FACTS, feedback linearization, nonlinear control, power system control.

1. INTRODUCTION

Stabilization of a synchronous generator is undoubtedly one of the most important problems in power system control. Power system stabilizers (PSS) and Automatic voltage regulators (AVR) with exciter are normally employed to damp out the electromechanical oscillations as well as for the post-fault bus-voltage recovery. However, it is well known that the performances of PSS and AVR are limited since their designs are primarily based on linear control algorithms. In the event of large faults, the nonlinearities of the system become very severe, thereby putting limitations on the performances of classical control designs. Thus, the most appropriate approach for controller design for a power system is the use of nonlinear control theory, i.e., multivariable feedback linearization scheme. The application of feedback linearization approaches for power system control was first investigated by Marino [1] and subsequently by several researchers [2-4]. This control

technique has also been successfully applied to control of drives and power electronics based systems [5-7].

The advent of advanced power electronics technology has enabled the use of voltage source inverters (VSI) at both the transmission and distribution levels. A number of VSI based systems such as STATCOM, Unified Power Flow Controller (UPFC), and Dynamic Voltage Restorer (DVR) has made FACTS possible. Successful applications of FACTS equipment for power flow control, voltage control and transient stability improvement have been reported in the literature [8-12].

This paper focuses on the use of STATCOM with a nonlinear controller for transient stability improvement and voltage control of power system. The fundamental principle of STATCOM is the generation of a controllable AC voltage source by a VSI connected to a DC Capacitor. The AC voltage source appears behind a transformer leakage reactance. The active and reactive power transfer is caused by the voltage difference across this reactance. The AC voltage

control is achieved by firing angle control. In steady state, the DC side capacitance is maintained at a fixed voltage and there is no real power exchange, except for losses. There are two control objectives in STATCOM control, i.e., AC-bus voltage control and DC voltage control across the capacitor. There are two voltage regulators designed for this purpose: AC bus voltage regulators and DC voltage regulator. Conventionally, both the regulators are proportional-integral (PI) type cascaded controllers [13, 14]. The modelling and control design are usually carried out in the standard synchronous $d-q$ frame [15]. Although, the cascade control structure yields good performance, it is not very much effective for all operating conditions because of the unsuitability of one set of PI gains for all four regulators of the cascade controllers and the inherent coupling between the d - and q - axis. In essence, since the complete model is highly nonlinear, the linear approach obviously does not offer better dynamic decoupling.

This work deals with the design of a nonlinear multivariable control technique for STATCOM using feedback linearization approach [16]. The feedback linearization technique is based on the idea of canceling the nonlinearities of the system and imposing a desired linear dynamics to control the system. The design has been tested by computer simulations under various types of large disturbances occurring in a single-machine infinite-bus power system equipped with AVR, exciter and PSS. The comparison of the results with conventional cascaded control structure of STATCOM reveals the supremacy of the feedback linearization control of STATCOM.

The remainder of the paper is organized as follows. The modelling of synchronous generator along with AVR, exciter and PSS, modeling of STATCOM, and the conventional cascade control scheme of a STATCOM have been described in Section 2 accompanied by a study of the simulation results under transient disturbance. Section 3 deals with the design of the proposed feedback linearizing nonlinear controller for STATCOM followed by a comparative evaluation of this new controller's performance via computer simulation results. Finally, the conclusions of this study are reported. The various parameters of the power system and the controllers are listed in the Appendix.

2. MATHEMATICAL MODELS AND CONVENTIONAL CONTROL SCHEMES

Figure 1 shows the single-machine infinite-bus power system considered in this work. An induction motor load and a STATCOM are connected at the load bus located between the generator bus and the infinite-bus. The mathematical models for the system components along with their control systems are described in the followings. The nomenclature is provided in the Appendix.

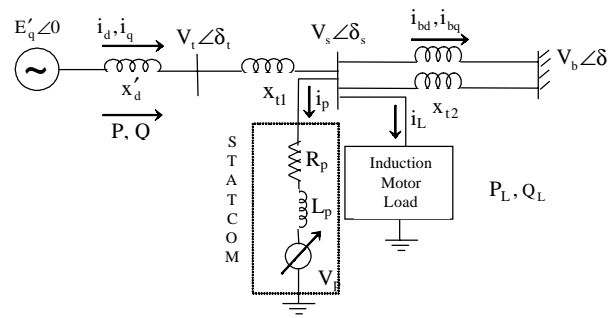


Fig. 1 A single-machine infinite-bus power system with a STATCOM connected to the load bus

2.1 Synchronous generator and speed governor

The synchronous generator is described by a third-order nonlinear mathematical model [17, 18]:

$$\frac{d\delta}{dt} = \Delta\omega \tag{1}$$

$$\frac{d\Delta\omega}{dt} = \frac{1}{M} [P_m - E'_q i_q - (x_q - x'_d) i_d i_q] \tag{2}$$

$$\frac{dE'_q}{dt} = \frac{1}{T'_{do}} [E_{fd} - E'_q - (x_d - x'_d) i_d] \tag{3}$$

$$\frac{d\Delta P_v}{dt} = [-\Delta P_v - K_g \Delta\omega + u_g] \tag{4}$$

$$\frac{d\Delta P_t}{dt} = [\Delta P_v - \Delta P_t] \tag{5}$$

where $\Delta\delta = \delta - \delta_0$ and $\Delta\omega = \omega - \omega_0$.

2.2 AVR, exciter and PSS

The excitation system of the generator consists of a simple automatic voltage regulator (AVR) and an exciter along with a supplementary power system stabilizer (PSS). The complete AVR+exciter+PSS control system is shown in Figure 2.

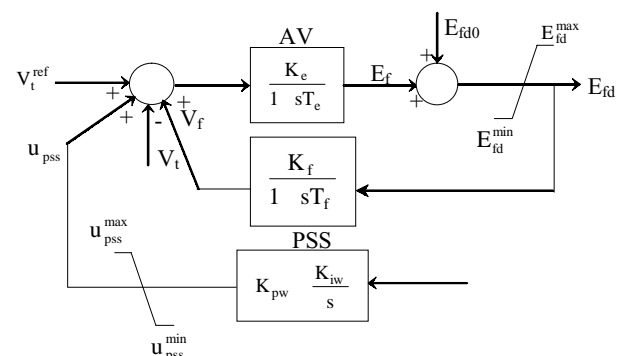


Fig. 2 AVR, exciter and PSS control system of the generating system

2.3 STATCOM

Figure 3 shows the basic structure of a 6-pulse STATCOM connected to a load bus in a power system where R_p represents the ‘ON’ state resistance of the switches including transformer leakage resistance, L_p is transformer leakage inductance and the switching losses are taken into account by a shunt dc -side resistance R_{dc} . A VSI resides at the core of the STATCOM. It generates a balanced and controlled 3-phase voltage V_p . The voltage control is achieved by firing angle control of the VSI. Under steady state, the dc -side capacitor possesses fixed voltage V_{dc} and there is no real power transfer, except for losses. Thus, the AC-bus voltage remains in phase with the fundamental component of V_p . However, the reactive power supplied by STATCOM is either inductive or capacitive depending upon the relative magnitude of fundamental component of V_p with respect to V_s . If $|V_s| > |V_p|$, the VSI draws reactive power from the AC-bus whereas if $|V_s| < |V_p|$, it supplies reactive power to the AC-system.

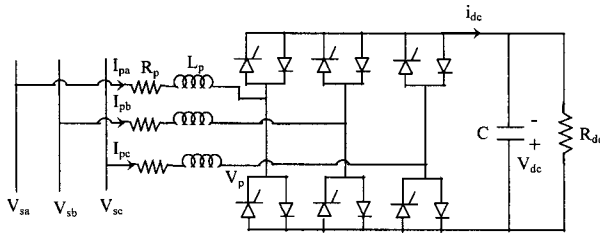


Fig. 3 Basic STATCOM connected to the load bus

2.3.1 Modeling of the STATCOM

The dynamic equations governing the instantaneous values of the three-phase voltages across the two sides of STATCOM and the current flowing into it are given by:

$$\left(R_p + L_p \frac{d}{dt} \right) \mathbf{i}_p = \mathbf{V}_s - \mathbf{V}_p \quad (6)$$

where:

$$\begin{aligned} \mathbf{i}_p &= [i_{pa} \ i_{pb} \ i_{pc}]^T, \\ \mathbf{V}_s &= [V_{sa} \ V_{sb} \ V_{sc}]^T, \\ \mathbf{V}_p &= [V_{pa} \ V_{pb} \ V_{pc}]^T, \end{aligned}$$

$$\mathbf{R}_p = \begin{bmatrix} R_p & 0 & 0 \\ 0 & R_p & 0 \\ 0 & 0 & R_p \end{bmatrix} \text{ and } \mathbf{L}_p = \begin{bmatrix} L_p & 0 & 0 \\ 0 & L_p & 0 \\ 0 & 0 & L_p \end{bmatrix} \quad (7)$$

Under the assumption that the system has no zero sequence components, all currents and voltages can be uniquely represented by equivalent space phasors [19] and then transformed into the synchronous d - q -

frame by applying the following transformation (θ is the angle between the d -axis and reference phase axis):

$$\mathbf{T} = \sqrt{\frac{2}{3}} \begin{bmatrix} \cos \theta & \cos \left(\theta - \frac{2\pi}{3} \right) & \cos \left(\theta + \frac{2\pi}{3} \right) \\ -\sin \theta & -\sin \left(\theta - \frac{2\pi}{3} \right) & -\sin \left(\theta + \frac{2\pi}{3} \right) \\ \frac{1}{\sqrt{2}} & \frac{1}{\sqrt{2}} & \frac{1}{\sqrt{2}} \end{bmatrix} \quad (8)$$

Thus, the transformed dynamic equations are:

$$\frac{di_{pd}}{dt} = -\frac{R_p}{L_p} i_{pd} + \omega i_{pq} + \frac{1}{L_p} (V_{sd} - V_{pd}) \quad (9)$$

$$\frac{di_{pq}}{dt} = -\omega i_{pd} - \frac{R_p}{L_p} i_{pq} + \frac{1}{L_p} (V_{sq} - V_{pq}) \quad (10)$$

where ω is the angular frequency of the AC-bus voltage.

It is to be noted that in the d - and q -axis components of the VSI voltage, i.e., V_{pd} and V_{pq} , all harmonics, which are near to/above the VSI switching frequency, are neglected. In the real-time implementation of these quantities, they should be converted into modulation index (m) and phase angle (ϕ):

$$m = \frac{\sqrt{V_{pd}^2 + V_{pq}^2}}{kV_{dc}}$$

and:

$$\phi = \tan^{-1} \left(\frac{V_{pq}}{V_{pd}} \right) \quad (11)$$

where k is a constant whose amplitude depends upon the adopted modulation technique.

For an effective DC-voltage control, the input power should be equal to the sum of load power (if any) and the charging rate of capacitor voltage on an instantaneous basis. Thus, by power balance between the AC input and the DC output:

$$\begin{aligned} p &= [V_{sd} i_{pd} + V_{sq} i_{pq} - (i_{pd}^2 + i_{pq}^2) R_p] = \\ &= CV_{dc} \frac{dV_{dc}}{dt} + \frac{V_{dc}^2}{R_{dc}} \end{aligned} \quad (12)$$

Hence:

$$\frac{dV_{dc}}{dt} = \frac{V_{sd} i_{pd} + V_{sq} i_{pq} - (i_{pd}^2 + i_{pq}^2) R_p}{CV_{dc}} - \frac{V_{dc}}{CR_{dc}} \quad (13)$$

Equation (13) models the dynamic behaviour of the dc -side capacitor voltage. In essence, Eqs. (9), (10) and (13) together describe the dynamic model of the STATCOM what is summarized for readiness in the next equation:

$$\frac{d}{dt} \begin{bmatrix} i_{pd} \\ i_{pq} \\ V_{dc} \end{bmatrix} = \begin{bmatrix} -\frac{R_p}{L_p} i_{pd} + \omega i_{pq} \\ -\frac{R_p}{L_p} i_{pq} - \omega i_{pd} \\ \frac{1}{CV_{dc}} [V_{sd} i_{pd} + V_{sq} i_{pq} - (i_{pd}^2 + i_{pq}^2) R_p] - \frac{V_{dc}}{CR_{dc}} \end{bmatrix} + \begin{bmatrix} \frac{1}{L_p} & 0 \\ 0 & \frac{1}{L_p} \\ 0 & 0 \end{bmatrix} \begin{bmatrix} V_{sd} - V_{pd} \\ V_{sq} - V_{pq} \end{bmatrix} \quad (14)$$

2.3.2 Cascade control scheme for STATCOM

The conventional control strategy for STATCOM concerns with the control of *ac*-bus and *dc*-bus voltage on both sides of STATCOM. The dual control objectives are met by generating appropriate current reference (for *d*- and *q*- axis) and, then, by regulating those currents in the STATCOM. PI controllers are conventionally employed for both the tasks while attempting to decouple the *d*- and *q*- axis current regulators. In this study, the strategy adopted by Padiyar et al. [14] and Schauder et al. [15] for shunt current control has been taken. The STATCOM current (i_p) is split into real (in phase with *ac*-bus voltage) and reactive components. The reference value for the real current is decided so that the capacitor voltage is regulated by power balance. The reference for reactive component is determined by *ac*-bus voltage regulator. As per the strategy, the original currents in *d-q* frame (i_{pd} and i_{pq}) are now transformed into another frame, *d'-q'* frame, where *d'*- axis coincides with the *ac*-bus voltage (V_s), as shown in Figure 4.

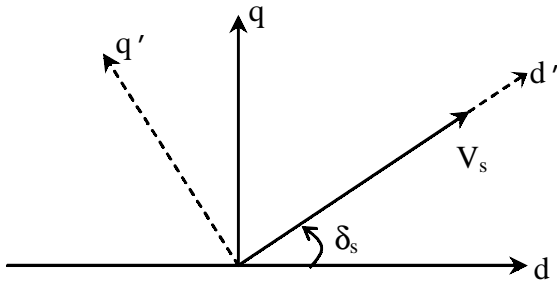


Fig. 4 Phasor diagram showing *d-q* and *d'-q'* frames

Thus, in *d'-q'* frame, the currents $i_{pd'}$ and $i_{pq'}$ represent the real and reactive currents and they are given by:

$$i_{pd'} = i_{pd} \cos \delta_s + i_{pq} \sin \delta_s \quad (15)$$

$$i_{pq'} = i_{pq} \cos \delta_s - i_{pd} \sin \delta_s \quad (16)$$

Now, for STATCOM current control, the differential equations (9) and (10) are reexpressed as:

$$\frac{di_{pd'}}{dt} = -\frac{R_p}{L_p} i_{pd'} + \bar{\omega} i_{pq'} + \frac{1}{L_p} (V_s - V_{pd'}) \quad (17)$$

$$\frac{di_{pq'}}{dt} = -\bar{\omega} i_{pd'} - \frac{R_p}{L_p} i_{pq'} + \frac{1}{L_p} (-V_{pq'}) \quad (18)$$

where:

$$V_{pd'} = V_{pd} \cos \delta_s + V_{pq} \sin \delta_s \quad (19)$$

$$V_{pq'} = V_{pq} \cos \delta_s - V_{pd} \sin \delta_s \quad (20)$$

$$\bar{\omega} = \omega + \frac{d\delta_s}{dt} \quad (21)$$

The VSI voltages are controlled as follows:

$$V_{pq'} = -(\bar{\omega} L_p i_{pd'} + L_p u_{q'}) \quad (22)$$

$$V_{pd'} = \bar{\omega} L_p i_{pq'} + V_s - L_p u_{d'} \quad (23)$$

By putting the above expressions for $V_{pd'}$ and $V_{pq'}$ in Eqs. (17) and (18), the following set of decoupled equations are obtained:

$$\frac{di_{pd'}}{dt} = -\frac{R_p}{L_p} i_{pd'} + u_{d'} \quad (24)$$

$$\frac{di_{pq'}}{dt} = -\frac{R_p}{L_p} i_{pq'} + u_{q'} \quad (25)$$

Also, the *dc*-bus voltage dynamic equation is now modified as:

$$\frac{dV_{dc}}{dt} = \frac{V_s i_{pd'} - (i_{pd'}^2 + i_{pq'}^2) R_p}{CV_{dc}} - \frac{V_{dc}}{CR_{dc}} \quad (26)$$

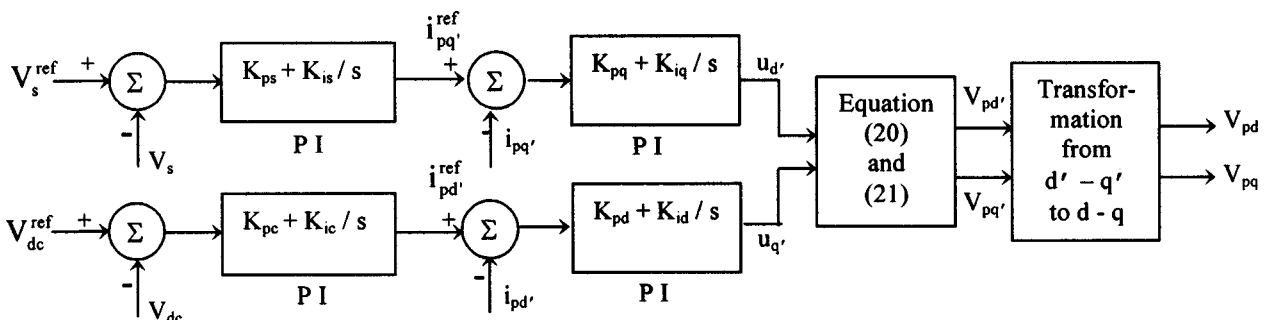


Fig. 5 Cascade control architecture for STATCOM control

Now, the control signals u_d' and u_q' can be easily determined by linear PI controllers. The complete cascade control architecture is shown in Figure 5 where K_{ps} , K_{is} , K_{pc} , K_{ic} , K_{pq} , K_{iq} , K_{pd} and K_{id} are the respective gains of the PI controllers.

2.4 Simulation results

The performance of the STATCOM (with the cascade control architecture) for stabilization of synchronous generator is evaluated by computer simulation studies. In the simulation studies, an induction motor load has been connected in the STATCOM bus. The load model is presented in the Appendix. The transient performances of the rotor angle, rotor speed deviation and bus voltages are compared in Figure 6 for a step change in induction motor load torque when the generator is operating at point $P=1 p.u.$ and $Q=0.2 p.u.$. Figure 7 shows the transient response of dc -bus voltage and the STATCOM control voltage. This paper clearly indicates better stabilizing properties of STATCOM, particularly the restoration of bus voltages to the pre-disturbance value.

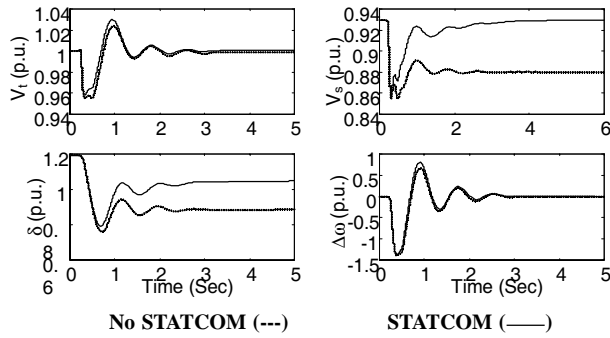


Fig. 6 Comparison of transient performance for induction motor load torque change ($P=1 p.u.$, $Q=0.2 p.u.$)

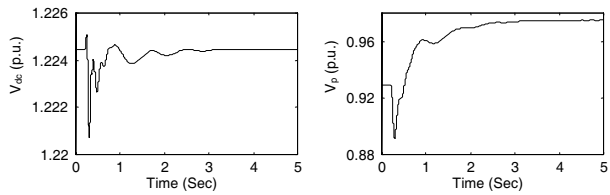


Fig. 7 Transient response of dc -bus voltage (V_{dc}) and the control voltage (V_p) for the induction motor load torque change ($P=1.0 p.u.$, $Q=0.2 p.u.$)

The cascade control approach leads to good control as illustrated by the above simulation results. However, it must be emphasized here that the decoupling approach taken in the above is not able to decouple the d - q components completely because of the coupled Eqs. (22) and (23) and, finally, in the frame transformation from d' - q' to d - q . Moreover, there are several PI controller gains to be determined for an effective control on the complete system. This obviously demands a lot of trial and error approach.

Further, the above decoupling technique does not take into account the coupling through the DC -capacitor voltage. All these difficulties always demand better and deeper modern control engineering approach. Such an approach using feedback linearization has been proposed in this paper. This technique attempts to linearize the system by nonlinear transformation and the complete STATCOM system is viewed as a whole for the control design. The details of the design algorithm are described in the following section.

3. FEEDBACK LINEARIZING NONLINEAR CONTROL OF STATCOM

In this section, the design steps for the feedback linearizing control of STATCOM have been presented followed by simulation results under various transient disturbances. A brief review of nonlinear control using feedback linearization [16] is presented in the Appendix.

3.1 Nonlinear control design

As mentioned earlier, in the STATCOM control, there are two broad objectives, i.e., ac -bus voltage (V_s) and dc -bus voltage (V_{dc}) control. In the following control design, V_s is taken as an additional state in addition to the other three states (i_{pd} , i_{pq} and V_{dc}) in the STATCOM modelling. The dynamic equation for V_s is obtained as follows with reference to Figure 4 (in the d' - q' frame):

$$V_s = V_{td'} + x_{t1}(i_{pq'} + i_{bq'} + i_{lq'}) \quad (27)$$

$$\frac{dV_s}{dt} = \frac{dV_{td'}}{dt} + x_{t1} \frac{d}{dt}(i_{lq'} + i_{bq'}) - \left(\frac{x_{t1} R_p}{L_p} \right) i_{pq'} - x_{t1} \bar{\omega} i_{pd'} - \left(\frac{x_{t1}}{L_p} \right) V_{pq'} \quad (28)$$

Now, for the control design, the complete state space model is expressed in the form of Eqs. (A.1) and (A.2) as follows:

$$\mathbf{x} = \begin{bmatrix} x_1 \\ x_2 \\ x_3 \\ x_4 \end{bmatrix} = \begin{bmatrix} i_{pd'} \\ i_{pq'} \\ V_{dc} \\ V_s \end{bmatrix} \quad \mathbf{u} = \begin{bmatrix} u_1 \\ u_2 \end{bmatrix} = \begin{bmatrix} -V_{pd'} \\ -V_{pq'} \end{bmatrix} \quad (29)$$

$$\dot{x}_1 = f_1(\mathbf{x}) + g_{11}u_1 \quad (30)$$

$$\dot{x}_2 = f_2(\mathbf{x}) + g_{22}u_2 \quad (31)$$

$$\dot{x}_3 = f_3(\mathbf{x}) \quad (32)$$

$$\dot{x}_4 = f_4(\mathbf{x}) + g_{41}u_1 + g_{42}u_2 \quad (33)$$

where:

$$f_1(\mathbf{x}) = -\frac{R_p}{L_p} x_1 + \bar{\omega} x_2 + \frac{1}{L_p} x_4 \quad (34)$$

$$g_1 = \frac{I}{L_p} = g_2 \quad (35)$$

$$f_2(\mathbf{x}) = -\bar{\omega}x_1 - \frac{R_p}{L_p}x_2 \quad (36)$$

$$f_3(\mathbf{x}) = \frac{I}{Cx_3} [x_1x_4 - R_p(x_1^2 + x_2^2)] - \frac{x_3}{CR_{dc}} \quad (37)$$

$$f_4(\mathbf{x}) = \left[-\frac{x_{t1}R_p}{L_p} \right] x_2 - \bar{\omega}x_{t1}x_1 + \frac{dV_{id'}}{dt} + x_{t1} \frac{d(i_{lq'} + i_{bq'})}{dt} \quad (38)$$

$$g_{41} = 0, \quad g_{42} = \frac{x_{t1}}{L_p} \quad (39)$$

The outputs of the system are V_s and V_{dc} .

Thus, $y_1 = V_s$ and $y_2 = V_{dc}$.

Proceeding with the exact steps as outlined in the Appendix, the following can be derived:

$$\begin{aligned} \begin{bmatrix} \dot{y}_1 \\ \dot{y}_2 \end{bmatrix} &= \begin{bmatrix} f_4(\mathbf{x}) \\ a_{11}f_1(\mathbf{x}) + a_{12}f_2(\mathbf{x}) + a_{13}f_3(\mathbf{x}) + a_{14}f_4(\mathbf{x}) \end{bmatrix} + \\ &+ \begin{bmatrix} g_{41} & g_{42} \\ a_{11}g_1 + a_{14}g_{41} & a_{12}g_2 + a_{14}g_{42} \end{bmatrix} \begin{bmatrix} u_1 \\ u_2 \end{bmatrix} = \\ &= \mathbf{A}(\mathbf{x}) + \mathbf{E}(\mathbf{x}) \begin{bmatrix} u_1 \\ u_2 \end{bmatrix} \end{aligned} \quad (40)$$

where:

$$a_{11} = \frac{I}{2Cx_3} (x_4 - 2R_p x_1) \quad (41)$$

$$a_{12} = -\frac{2R_p x_2}{Cx_3} \quad (42)$$

$$a_{13} = \frac{I}{x_3} \left[R_p (x_1^2 + x_2^2) - x_1 x_4 \right] - \frac{I}{CR_{dc}} \quad (43)$$

$$a_{14} = \frac{x_1}{Cx_3} \quad (44)$$

Thus:

$$\begin{bmatrix} u_1 \\ u_2 \end{bmatrix} = \mathbf{E}^{-1}(\mathbf{x}) \left[-\mathbf{A}(\mathbf{x}) + \begin{bmatrix} v_1 \\ v_2 \end{bmatrix} \right] \quad (45)$$

The nonsingularity of $\mathbf{E}(\mathbf{x})$ can be observed by computing the determinant of $\mathbf{E}(\mathbf{x})$, which is:

$$|\mathbf{E}(\mathbf{x})| = -\frac{x_{t1}}{CL_p^2} \left(\frac{V_s - 2R_p i_{pd'}}{V_{dc}} \right) \quad (46)$$

It is known that the magnitude of current $i_{pd'}$ is very small such that $2R_p i_{pd'}$ is almost negligible compared to V_s . Now it is readily seen that $\mathbf{E}(\mathbf{x})$ is nonsingular in the operating ranges of V_s and V_{dc} .

For tracking of V_s and V_{dc} , the new control inputs v_1 and v_2 are selected as (by both proportional and integral control):

$$\begin{bmatrix} v_1 \\ v_2 \end{bmatrix} = \begin{bmatrix} \dot{y}_{1ref} + K_{11}e_1 + K_{12} \int e_1 dt \\ \ddot{y}_{2ref} + K_{21}\dot{e}_2 + K_{22}e_2 + K_{23} \int e_2 dt \end{bmatrix} \quad (47)$$

where y_{1ref} is the ac-bus reference voltage (V_s^{ref}) and y_{2ref} is the dc-bus reference voltage (V_{dc}^{ref}) and e_1 and e_2 are error variables defined by:

$$e_1 = V_s^{ref} - V_s$$

and:

$$e_2 = V_{dc}^{ref} - V_{dc} \quad (48)$$

From Eq. (48), the error dynamics is given by:

$$\ddot{e}_1 + K_{11}\dot{e}_1 + K_{12}e_1 = 0 \quad (49)$$

$$\ddot{e}_2 + K_{21}\dot{e}_2 + K_{22}e_2 + K_{23}e_2 = 0 \quad (50)$$

The gain parameters K_{11} , K_{12} , K_{21} , K_{22} and K_{23} are determined by assigning desired poles on the left-half s -plane and, thus, asymptotic tracking control to the reference can be achieved. From u_1 and u_2 , the control signals in d' - q' frame are determined by:

$$V_{pd'} = -u_1$$

and:

$$V_{pq'} = -u_2 \quad (51)$$

Again, from $V_{pd'}$ and $V_{pq'}$, the control signals in d - q frame i.e., V_{pd} and V_{pq} , are obtained by making use of Eqs. (19) and (20).

In the computer simulation studies presented in the followings, the derivative $dv_{id'}/dt$ appearing in the control design, i.e., Eqs. (29) and (39), is neglected in the control computation. This leads to the assumption that the generator bus voltage V_t is treated as a constant only for the control design. In the complete simulation of the nonlinear system, V_t varies as per the system conditions. It is emphasized that, by neglecting $dv_{id'}/dt$ exclusively for the control computation, any unusual rise in the control signal is avoided under severe transient conditions, i.e., 3-phase fault, which may lead to instability depending upon the operating point. Further, because of the direct non-availability of rotor speed deviation ($\Delta\omega$) at the load bus, the nominal frequency ω_0 has been used in the control calculations. Thus, although the nonlinear control design becomes a suboptimal one because of the above constraints in the control computation, its feasibility is very much practical as presented in the followings.

3.2 Simulation results

The above feedback linearizing (FL) control algorithm for STATCOM is evaluated by computer simulation studies under various transient conditions. In the simulation experiment, $dv_{id'}/dt$ is neglected as discussed earlier. A comparison of the system responses for a 3-phase fault at infinite bus ($P=1.0$ p.u., $Q=0.2$ p.u.) which is cleared after 0.1 sec is shown in Figure 8.

The transient oscillations in rotor angle and speed exhibit good damping behaviour for feedback linearizing controller compared to cascade PI controllers. This is possible because of efficient nonlinear control of bus voltage, resulting in better power modulation, by the feedback linearizing controller for stabilizing the synchronous generator.

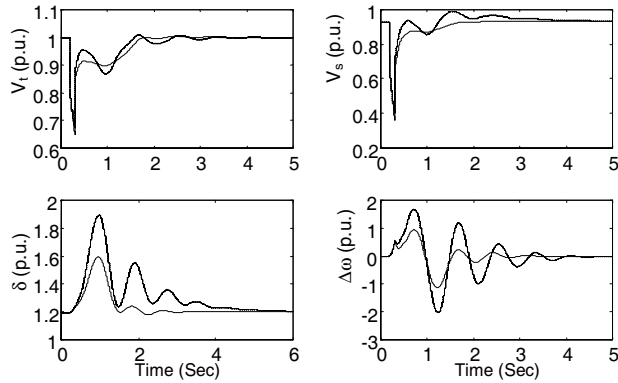


Fig. 8 Comparison of transient performance for a 3-phase fault at infinite bus ($P=1.0$ p.u., $Q=0.2$ p.u.); FL (—), PI (---)

Similar damped oscillations are also seen in the case of 10% change in governor input, also, for the case of 50% line switching between the load bus and infinite bus for the same operating point ($P=1.0$ p.u., $Q=0.2$ p.u.). The results are displayed in Figures 9 and 10, respectively.

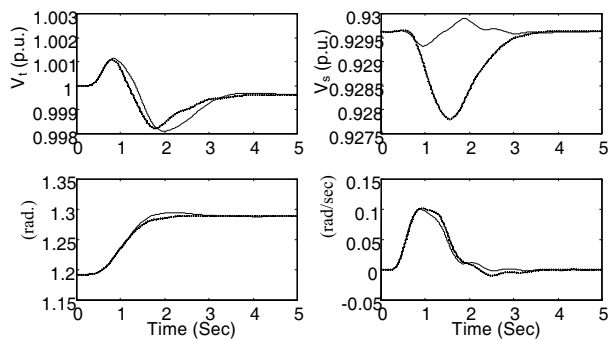


Fig. 9 Comparison of transient performance for 10% increase in governor input ($P=1.0$ p.u., $Q=0.2$ p.u.); FL (—), PI (---)

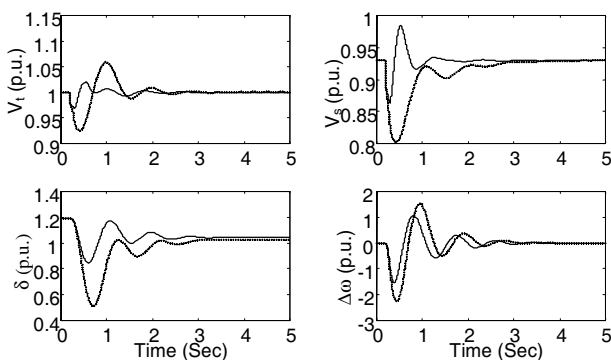


Fig. 10 Comparison of transient performance for 50% line switching ($P=1.0$ p.u., $Q=0.2$ p.u.); FL (—), PI (---)

As an additional illustration, Figure 11 illustrates the superior performance of FL controller for a 3-phase fault at infinite bus and cleared after 0.1 sec at a different operating point ($P=0.8$ p.u., $Q=0.4$ p.u.).

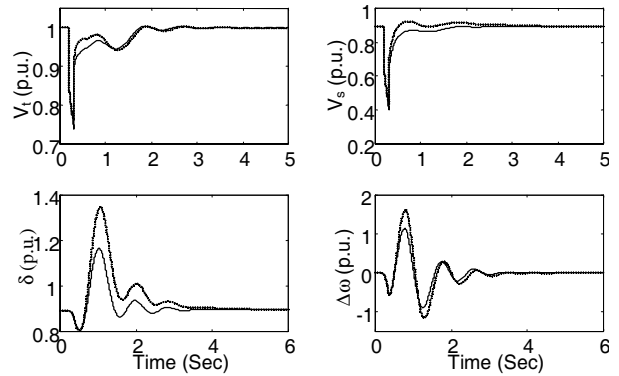


Fig. 11 Comparison of transient responses for a 3-phase fault at infinite bus ($P=0.8$ p.u., $Q=0.4$ p.u.); FL (—), PI (---)

Further to highlight the superiority of the proposed FL controller for wide operating ranges, a 3-phase fault is created at the infinite bus for a leading power factor condition ($P=0.8$ p.u., $Q=-0.2$ p.u.) for a duration of 0.1 sec. It is observed that the same PI gains leads to an instability of the system where as the FL controller stabilizes the system. The results are reported in Figure 12.

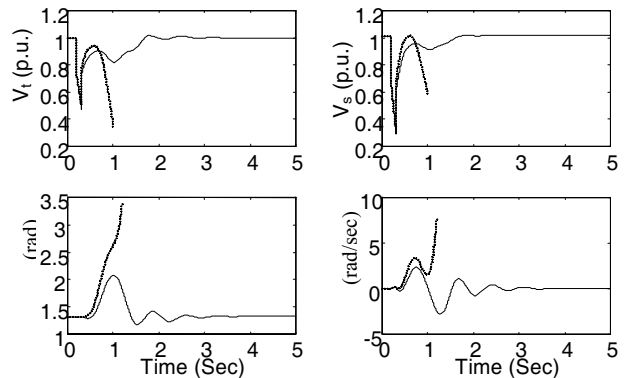


Fig. 12 Comparison of transient responses for a 3-phase fault at infinite bus ($P=0.8$ p.u., $Q=-0.2$ p.u.); FL (—), PI (---)

All the above simulation results demonstrate the superior performance of the proposed FL controller over the cascaded PI controller for large disturbances like 3-phase fault, change in mechanical power and line switching. For the simulation of a relatively smaller disturbance, the induction motor load torque is changed 2.5 times and the simulation results are presented in Figure 13. In all the case studies presented above, the feedback linearizing control of STATCOM provides excellent damping for the electromechanical transient oscillations of the synchronous generator compared to the conventional cascade control of STATCOM.

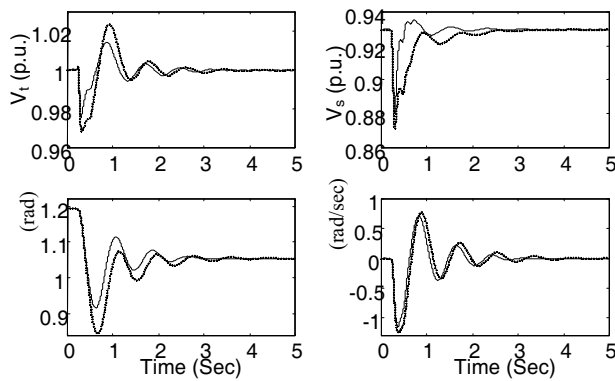


Fig. 13 Comparison of transient responses for induction motor load torque change by 2.5 times ($P=1.0$ p.u., $Q=0.2$ p.u.); FL (—), PI (---)

4. CONCLUSIONS

A step-by-step approach has been presented for the design of a nonlinear controller based on feedback linearization for STATCOM and an induction motor load connected to the load bus of a single-machine infinite-bus power system. The novelty of this approach is that the nonlinearity appearing in the STATCOM model is eliminated by feedback linearization, thereby, allowing the applicability of a linear control law obtained via pole placement. As illustrated by computer simulation studies, the superior damping of the electromechanical oscillations of the synchronous generator provided by this proposed control strategy over the conventional cascade control approach has been established for a variety of severe transient disturbances.

As of present design methodology, the poles are placed at fixed locations for all operating points of the synchronous generator. An attractive and effective approach will be to allow provisions for adaptive pole placement. This aspect is currently under investigation by the authors.

5. REFERENCES

- [1] R. Marino, An example of a nonlinear regulator, *IEEE Transactions on Automatic Control*, Vol. AC-29, No. 3, pp. 276-279, 1984.
- [2] J.W. Chapman, M.D. Ilic, C.A. King, L. Eng and H. Kaufman, Stabilizing a multimachine power system via decentralized feedback linearizing excitation control, *IEEE Transactions Power Systems*, Vol. 8, No. 3, 1993.
- [3] W. Mielczarski and A.M. Zajaczkowski, Multivariable nonlinear controller for a synchronous generator, *Optimal Control Applications and Methods*, Vol. 15, pp. 49-65, 1994.
- [4] O. Akhrif, F.A. Okou, L.A. Dessaint and R. Champagne, Application of a multivariable feedback linearization scheme for rotor angle stability and voltage regulation of power systems, *IEEE Transactions on Power Systems*, Vol. 14, No. 2, pp. 620-628, 1999.
- [5] H. Sira-Ramirez and M. Ilic-Spong, Exact linearization in switched-mode DC to DC power converters, *International Journal of Control*, Vol. 50, No. 2, pp. 511-524, 1989.
- [6] D.I. Kim, I.J. Ha and M.S. Ko, Control of induction motor via feedback linearization with input-output decoupling, *International Journal of Control*, Vol. 51, No. 4, pp. 863-886, 1990.
- [7] Y.L. Tan and Y. Wang, Design of series and shunt FACTS controller using adaptive nonlinear coordinated design techniques, *IEEE Transactions on Power Systems*, Vol. 12, No. 3, pp. 1374-1379, 1997.
- [8] L. Gyugyi, Dynamic compensation of AC transmission lines by solid-state synchronous voltage sources, *IEEE Transactions on Power Delivery*, Vol. 9, pp. 904-911, 1994.
- [9] R. Mihalić, P. Žunko, I. Papić and D. Povh, Improvement of transient stability by insertion of FACTS devices, *IEEE/NTUA Athens Power Tech. Conference Proc.*, pp. 521-525, 1993.
- [10] B.M. Han, G.G. Karady, J.K. Park and S.I. Moon, Interaction analysis model for transmission static compensator with EMTP, *IEEE Transactions on Power Delivery*, Vol. 13, No. 4, pp. 1297-1302, 1998.
- [11] P.W. Lehn and M.R. Irvani, Experimental evaluation of STATCOM closed loop dynamics, *IEEE Transactions on Power Delivery*, Vol. 13, No. 4, pp. 1378-1384, 1998.
- [12] S. Mori, K. Matsuno, M. Takeda and M. Seto, Development of a large static VAR generator using self-communicated inverters for improving power system stability, *IEEE Transactions on Power Systems*, Vol. 8, No. 1, pp. 371-378, 1993.
- [13] M. Mohaddes, A.M. Gole and P.G. McLaren, A neural network controlled optimal pulse-width modulated STATCOM, *IEEE Transactions on Power Delivery*, Vol. 14, No. 2, pp. 481-488, 1999.
- [14] K.R. Padiyar and A.M. Kulkarni, Control design and simulation of a unified power flow controller, *IEEE Transactions on Power Delivery*, Vol. 13, No. 4, pp. 1348-1354, 1998.
- [15] C. Schauder and H. Mehta, Vector analysis and control of advanced static VAR compensator, *IEE Proceedings - C*, Vol. 140, No. 4, pp. 299-306, 1993.
- [16] J.E. Slotine and W. Li, *Applied Nonlinear Control*, Prentice-Hall International Editions, pp. 207, 1991.
- [17] P.M. Anderson and A.A. Fouad, *Power System Control and Stability*, IEEE Press, New York, 1994.

- [18] A.R. Bergen, *Power System Analysis*, Prentice-Hall, New Jersey, 1986.
 [19] P. Vas, *Vector Control of AC Machines*, Oxford University Press, New York, 1990.
 [20] B.C. Lesieutre, P.W. Sauer and M.A. Pai, Development and comparative study of induction machine based dynamic P,Q load models, *IEEE Transactions on Power Systems*, Vol. 10, No. 1, pp. 182-191, 1995.

APPENDIX

A.1 Nomenclature

- δ – rotor angle with respect to the infinite bus system voltage
 M – effective inertia constant of synchronous generator
 E_q' – ransient q -axis voltage
 x_d – d -axis reactance
 x_q – q -axis reactance
 x_d' – d -axis transient reactance
 E_{fd} – direct excitation voltage
 T_{do}' – equivalent transient rotor time constant
 ΔP_t – deviation of turbine output
 ΔP_v – deviation of valve opening position

The valve opening or closing speed is restricted by:

$$\frac{d\Delta P_v}{dt} \leq P_{vmax} \text{ where } P_{vmax} \text{ is specified to be } 0.1 \text{ p.u./sec}$$

in the simulation.

- u_g – governor input command
 P, Q – active and reactive power
 R_s – stator resistance of the induction motor
 R_r – rotor resistance of the induction motor
 X_s – stator reactance of the induction motor
 X_r – rotor reactance of the induction motor
 X_m – mutual reactance of the induction motor
 H_m – moment of inertia of induction motor
 K_e and T_e – AVR gain and time constants
 K_f and T_f – exciter gain and time constants
 K_g and T_g – governor gain and time constants
 T_t – turbine time constant

The subscript 0 indicates the initial value of the variable.

A.2 Feedback linearizing control

A brief review of nonlinear control using feedback linearization [16] is presented here. Without loss of generality, the following MIMO system is considered:

$$\dot{x} = f(x) + g(x)u \tag{A.1}$$

$$y = h(x) \tag{A.2}$$

where $x(\in \mathfrak{R}^n)$ is state vector, $u(\in \mathfrak{R}^m)$ represents control inputs, $y(\in \mathfrak{R}^m)$ stands for output, f and g are smooth vector fields, and h is a smoth scalar function. The input-output linearization of the above MIMO system is achieved by differentiating y of the system until the outputs appear explicitly. Thus, by differentiating Eq. (A.2) we obtain:

$$\dot{y}_i = L_f h_i + \sum_{j=1}^m (L_{g_j} h_i) u_j, \quad i = 1, \dots, m \tag{A.3}$$

where $L_f h$ and $L_g h$ represent the L_{ie} derivatives of $h(x)$ with respect to $f(x)$ and $g(x)$, respectively. The key point is that, if $L_{g_j} L_f^{(r_i-1)} h_i(x) = 0$ for all j , then the inputs do not appear in Eq. (A.3) and further differentiation is to be repeated as:

$$y_i^{(r_i)} = L_f^{(r_i)} h_i + \sum_{j=1}^m (L_{g_j} L_f^{(r_i-1)} h_i) u_j, \quad i = 1, \dots, m \tag{A.4}$$

such that $L_{g_j} L_f^{(r_i-1)} h_i(x) \neq 0$ for at least one j . This procedure is repeated for each output y_i . Thus, there will be a set of m equations given by:

$$\begin{bmatrix} y_1^{(r_1)} \\ \vdots \\ y_m^{(r_m)} \end{bmatrix} = \begin{bmatrix} L_f^{r_1} h_1(x) \\ \vdots \\ L_f^{r_m} h_m(x) \end{bmatrix} + E(x) \begin{bmatrix} u_1 \\ \vdots \\ u_m \end{bmatrix} \tag{A.5}$$

where $E(x)$ is expressed by:

$$E(x) = \begin{bmatrix} L_{g_1} L_f^{r_1-1} h_1 & \dots & L_{g_m} L_f^{r_1-1} h_1 \\ \vdots & \ddots & \vdots \\ L_{g_1} L_f^{r_m-1} h_m & \dots & L_{g_m} L_f^{r_m-1} h_m \end{bmatrix} \tag{A.6}$$

$E(x)$ is suitably called as the decoupling matrix for the MIMO system. If $E(x)$ is nonsingular, then the control u can be obtained as:

$$u = -E^{-1}(x) \begin{bmatrix} L_f^{r_1} h_1(x) \\ \vdots \\ L_f^{r_m} h_m(x) \end{bmatrix} + E^{-1}(x) \begin{bmatrix} v_1 \\ \vdots \\ v_m \end{bmatrix} \tag{A.7}$$

where $[v_1 \dots v_m]^T$ are the new set of inputs defined by the designer. The resultant dynamics of the system with new control is easily obtained by substitution of Eq. (A.7) into Eq. (A.5) and is given by:

$$\begin{bmatrix} y_1^{(r_1)} \\ \vdots \\ y_m^{(r_m)} \end{bmatrix} = \begin{bmatrix} v_1 \\ \vdots \\ v_m \end{bmatrix} \tag{A.8}$$

It is readily noticed that the input-output relation in Eq. (A.8) is decoupled and linear.

A.3 Induction motor load model

A third order induction motor model [20] is taken as given bellow.

Stator

$$V_{sd} = E'_d - X I_{qs} \quad (A.9)$$

$$V_{sq} = E'_q - X I_{ds} \quad (A.10)$$

Rotor

$$T'_0 \frac{dE'_q}{dt} = -E'_q + \frac{X_m^2}{X_r} I_{ds} - s \frac{X_r}{R_r} E'_d \quad (A.11)$$

$$T'_0 \frac{dE'_d}{dt} = -E'_d + \frac{X_m^2}{X_r} I_{qs} - s \frac{X_r}{R_r} E'_q \quad (A.12)$$

Torque equation

$$2H_m \frac{ds}{dt} = T_L - (E'_q I_{qs} + E'_d I_{ds}) \quad (A.13)$$

The mechanical load torque is assumed to be proportional to rotor speed. Thus:

$$T_L = k_0 \omega_r = k_0 \omega_s (1-s) = k_L (1-s) \quad (A.14)$$

$$X' = \frac{X_s X_r - X_m^2}{X_r}, \quad T'_0 = \frac{X_r}{\omega_s R_r}, \quad s = \frac{\omega_s - \omega_r}{\omega_s}$$

where V_{sd} and V_{sq} correspond to voltages of the STATCOM-bus.

A.4 System parameters

Power System, AVR, exciter and PSS:

$$\begin{aligned} x_d &= 1.9 \text{ p.u.}, x_q = 1.6 \text{ p.u.}, x'_d = 0.17 \text{ p.u.}, \\ T_{do}' &= 4.314 \text{ sec}, \omega_0 = 100 \pi \text{ rad/sec}, \\ x_{t1} &= 0.2 \text{ p.u.}, x_{t2} = 0.2 \text{ p.u.}, M = 0.03 \text{ p.u.}, \\ K_e &= 200, T_e = 0.1 \text{ sec}, K_{pw} = 5, K_{iw} = 12, \\ E_{fd}^{max} &= 6 \text{ p.u.}, E_{fd}^{min} = -6 \text{ p.u.}, \\ u_{pss}^{max} &= 0.01 \text{ p.u.}, u_{pss}^{min} = -0.01 \text{ p.u.}, \\ K_g &= 0.067, T_g = 0.1 \text{ sec}, T_t = 0.3 \text{ sec}, \\ K_f &= 0.01, T_f = 0.5 \text{ sec}. \end{aligned}$$

Induction motor:

$$\begin{aligned} R_s &= 0.0079 \text{ p.u.}, x_s = 1.2287 \text{ p.u.}, \\ R_r &= 0.0053 \text{ p.u.}, x_r = 1.2233 \text{ p.u.}, x_m = 1.18 \text{ p.u.}, \\ H_m &= 0.41 \text{ p.u.} \end{aligned}$$

STATCOM:

$$\begin{aligned} R_p &= 0.04 \text{ p.u.}, \omega_0 L_p (= x_p) = 0.1 \text{ p.u.}, \\ R_{dc} &= 150, C = 5000 \mu F. \end{aligned}$$

Cascade PI controllers:

$$\begin{aligned} K_{ps} &= 1, K_{is} = 10, K_{pq} = 5, K_{iq} = 1666; \\ K_{pc} &= 0.1, K_{ic} = 1, K_{pd} = 50, K_{id} = 16667. \end{aligned}$$

Feedback linearizing controller:

Desired pole locations:

- For computation of K_{11} and K_{12} are:
 $s_1 = -0.2, s_2 = -0.2.$
- For computation of K_{21}, K_{22} and K_{23} are:
 $s_1 = -200, s_2 = -100, s_3 = -50.$

NELINEARNA KONTROLA STATCOM-A ZA STABILIZACIJU SINKRONOG GENERATORA

SAŽETAK

Statički sinkroni kompenzator (STATCOM) tipičan je fleksibilni AC prijenosni sustav (FACTS) odnosno uređaj koji ima važnu ulogu u postizanju stabilnosti malih i velikih prijelaznih poremećaja u međusobno spojenom energetskom sustavu. Ovaj rad se bavi projektiranjem i procjenom nelinearnog upravljačkog sklopa linearizirajuće povratne veze za STATCOM koji je instaliran na krutu mrežu energetskog sustava. Osim koordinirane kontrole AC i DC napona sabirnice predloženi regulator omogućava i dobro prigušenje elektromehaničke oscilacije ovog sinkronog generatora pod prijelaznim poremećajima. Učinkovitost strategije kontrole procjenjuje se pomoću kompjuterski simuliranih studija. Komparativna studija ovih rezultata s konvencionalnom upravljačkom kaskadnom strukturom uočava prednosti predložene kontrolne sheme.

Ključne riječi: STATCOM, FACTS, linearizacija povratne veze, nelinearna kontrola, kontrola energetskog sustava.